DOI: https://doi.org/10.46354/i3m.2019.mas.015

A SIMULATION TOOL FOR MASS TRANSFER INSIDE COMPRESSED AIR VESSEL FOR WATER NETWORKS PRESSURISATION

Andrea Volpi [(a)], Eleonora Bottani [(b)]

[(a), (b)] Department of Engineering and Architecture, University of Parma (Italy)

(a) andrea.volpi@unipr.it, [(b)] eleonora.bottani@unipr.it

ABSTRACT

Feeding a water distribution network with the correct pressure is a fundamental requirement for its proper operation; to this end, a simple and reliable solution commonly adopted in small and medium industrial plants is the adoption of a pressure vessel. For small systems, a membrane seals the system water from the gas compartment, anyway, as the size of the vessel increases, the adoption of sealing diaphragm or bladder is no longer feasible, and thus there is a direct contact between air and water. The high pressure of the vessel, combined with the cyclic loading and unloading phases, which replace the water inside the tank, leads to a considerable mass transfer phenomenon of air inside water. The loss of air mass cannot be monitored and detected by simply controlling system pressures; to this extent, water level measurement and reference analytical models are required. Since there is a lack in scientific literature of these models, the present study presents a model for mass transfer estimate in the systems described, starting from a real pilot plant. The main results of the model implementation in a spreadsheet, in terms of the trend of the key model parameters in time, are also reported and discussed.

Keywords: pressure vessel, compressed air vessel, mass transfer, water pressurisation systems

1. INTRODUCTION

A correct pressure is the fundamental requirement for the proper operation of water distribution networks; to this end, a simple and reliable solution is the adoption of a pressure vessel. The vessel itself is independent on the electrical power and easy to operate. For small systems, a diaphragm seals the system water from the gas compartment, avoiding any contamination, corrosion and pressure loss. The result is a fully closed system that does not suffer from corrosion or other gas-related problems.

Pressurization stations are the further development of the traditional diaphragm expansion vessels for large volume and/or high-pressure systems. The principle differs because of the use of an additional control unit, which allows transferring the expansion volume to a separate expansion vessel. Due to the highly accurate control, the pressure changes in the system are kept to minimum.

Once connected to the water system, the pump starts to raise the pressure letting the water filling in the bladder. When the pressure reaches its maximum threshold value p_{MAX}, the pump stops. Inside the tank, there is the greatest quantity of water possible. Obviously, the membrane dilates and occupies almost all the volume of the tank. When water is required by the system, it starts flowing out of the tank without using the pump but just expanding the air cushion, whose pressure decreases.

The process goes on and the membrane deflates until the pressure reaches its minimal threshold value p_{MIN}. At this stage the membrane is back to its initial size, the pump starts working again and a new cycle begins. Since the pump always grants the maximum water flow, its insertions are kept to the minimum. Moreover, since air chambers show good ability in controlling the pressure surge from a water hammer (WH) phenomenon, compressed air vessel (CAV) is often adopted in a pressurized system for limiting pressure spikes. The system is very flexible; anyway, as the volume of water increases, the adoption of sealing diaphragm or bladder is no longer feasible, and thus there is a direct contact between air and water. The system still works as described above; therefore, the high pressure of the vessel, combined with the cyclic loading and unloading phase (replacing the water inside the tank), involves a mass transfer phenomenon of air inside water.

The aim of the presented work is to present an analytic model capable of representing the behaviour of the above-mentioned system, i.e. a pressure vessel in which air compression and mass transfer phenomena happen.

2. LITERATURE REVIEW

Many authors have investigated the behaviour of pressure vessels as a remedy for WH; Ivljanin et al. (2018) have used numerical simulation to describe the homogeneous two-phase flow model and a non-equilibrium system of air mass transfer between dispersed air bubbles and continuous liquid water during WH transient with gaseous cavitation.

Besharat et al. (2016) have simulated an air chamber and studied the behaviour of air inside it, with a CAV in a pressurized system. They carried out experimental tests, 1D and 2D computational fluid dynamics (CFD) simulations for an air pocket (AP) within a CAV in the case of rapid pressurization and the occurrence of WH in a pressurized system.

Again, Besharat et al. (2017) have studied an AP, confined in CAV, under several different WH events to

better define the use of protection devices or compressed air energy storage systems. This research focused on the size of an AP within an air vessel and tried to describe how it affects important parameters of the system, i.e., pressure in the pipe, stored pressure, flow velocity, displaced volume of water and water level in the CAV.
Zhou et al. (2011) have investigated the pressure variations associated with a filling undulating pipeline containing an entrapped AP both experimentally and numerically. The influence of entrapped air on abnormal transient pressures was often ambiguous because the compressibility of the air pocket allowed the liquid flow to accelerate but also partly cushioned the system, with the balance of these tendencies being associated with the initial void fraction of the AP.
Other studies have focused on the gas absorption phenomenon under different circumstances. Okayama et al. (2018) observed and calculated with CFD method plunging pool formation and gas absorption phenomena during tapping.
Vlyssides et al. (2003) have studied the transfer rate of air to water in a sparged agitated pressure vessel. The mass transfer coefficient of air was proved to depend on the mixing energy, the airflow rate as well as the vessel's pressure and temperature.
These studies represent just some examples of the topics investigated by the current literature; as it can be noticed the air cushion in CAV is often analysed in conjunction with WH or pressure transient, while mass transfer of gas is mentioned in several processes but not in steady pressure vessel for water. Hence, there is a lack in scientific literature of a model for water vessel equipped with an air cushion as a pressurisation system for a water distribution network, which is the object of the present study.
The paper is organised as follows: Section 3 (Materials and methods) describes the working principles of a real pilot pressure vessel system (3.1) and the key features of its components (3.2); then the analytical models without mass transfer (3.3) and with mass transfer (3.4) are deeply described. Section 4 presents the obtained results and, finally, Section 5 reports summarizing conclusions.

3. MATERIALS AND METHODS

3.1. Pressure vessel principles

In line with the purpose of this study, a small-scale pilot plant of a pressurisation system for a water distribution network was built and installed in a laboratory at the Department of Engineering and Architecture of the University of Parma. This plant was useful to observe a real system and represented the basis for the development of the simulation model, to ensure its realistic behaviour.
The pressure plant is represented in Figure 1; its main components are: (1) tank, (2) pump, (3) check valve, (4) CAV, (5) vessel supports, (6) level probe, (7) and (8) pressure probes, (9) level indicator, (10) safety valve, (11) interception valve, (12) compressed air inlet, (13) controller (PLC).

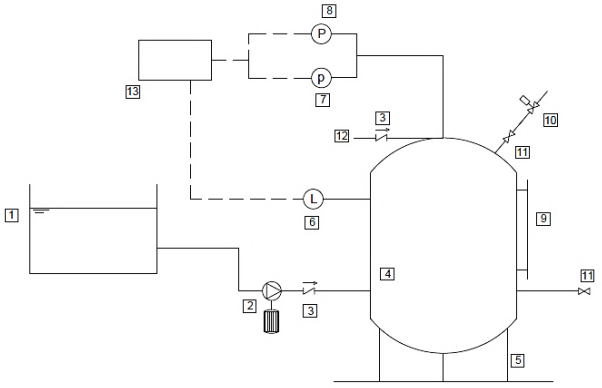

Figure 1: experimental setup.

At the beginning of the experiment, a small quantity of water is loaded in the vessel and then the CAV is pressurized by means of an external connection with compressed air distribution systems. The pressure of the air cushion inside the vessel is raised to the minimum value (p_{MIN}) required by the water distribution plant, when the minimum quantity of water is inside the vessel. The air volume obtained is referred as V_2.
Once the controller is turned on, the pump starts raising the pressure further, by letting the water filling in the vessel. When the pressure reaches its maximum threshold value (p_{MAX}), the pump stops. Inside the tank there is the greatest possible quantity of water, and the trapped air is compressed to its minimum volume V_1. At the water-air interface, mass transfer takes place and, due to the high air pressure, an amount of air passes into the water until the new maximum allowed concentration is reached.
If water is requested by the distribution network, it starts flowing out of the tank without using the pump but just expanding the air cushion, whose pressure decreases. The process goes on until the pressure reaches its minimum threshold value p_{MIN}; when this happens, the pump starts working again and a new cycle begins. It must be noticed that the air concentration of fresh water, pumped inside the vessel, is not balanced inside the CAV, due to the increased water pressure, and thus a mass transfer phenomenon of air solubilisation into water happens. Since the pump always grants the maximum water flow Q_{MAX}, its insertions are reduced to the minimum; in fact, the size of the vessel is intended to reduce to an acceptable value the switch-on cycles of the pump according to the starts per hour admitted by the electric motor.
The object of the present work is to simulate a finite number of operating cycles as described above, in order to point out the mass transfer phenomenon which takes place inside the CAV. In particular, the pressure vessel and the trend of compressed air mass (weight and composition) are studied as a function of required water flow of the distribution network over time. Intentionally, the influence of temperature on the system is neglected, since all the air transformations take place at a constant room (and water) temperature, equals to 25°C.

3.2. System description

Different elements compose the pressurization group described:

- layout elements like feeding tank, pressure vessel, valves, piping, centrifugal pump;
- monitoring system composed of pressure probes, flow meter, level gauge;
- actuators for water pump, compressed air input valve and distribution network output valve.

The pump, whose main features are presented in Table 1, is 12-volt powered and it supplies water inside the CAV; the water source is an external tank at atmospheric pressure (1 absolute atm or 1 ata). According to the datasheet of the pump, it is possible to obtain the characteristic curve, showing the delivered flow Q_{MAX} as a function of the operating voltage (volt) and discharge pressure.

Table 1: pump features.

Fuel pressure	5 bar or 8 bar (relative)
Delivery rate (5 bar, 25 C)	260 ± 5 l/h at 14 volt
Delivery rate (8 bar, 25 C)	220 ± 5 l/h at 14 volt
Pressure limiting valve	10 to 12.5 bar
Fuel compatibility	Up to E85 with shorter lifetime
Operating temperature range	-20 to +90 C
Storage temperature range	-40 to +70 C
Max vibration	3 mm at 10 to 18 Hz ≤40 m/s^2 at 18 to 60 Hz

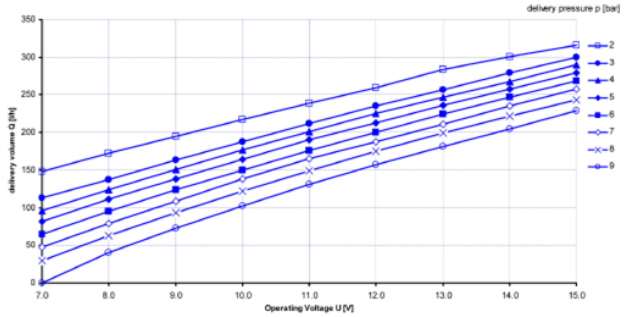

Figure 2: characteristic curve of the pump.

According to the maximum flow rate Q_{MAX} [*l/min*], it is also possible to determine the maximum number of pump switch-on per hour, indicated with *n*, according to the following equation:

$$n = \frac{30 * Q_{MAX}}{V_u} \left[\frac{switch-on}{hour}\right] \quad (1)$$

where V_u, given by V_2-V_1, represents the difference between the volume of water at p_{MIN} and the volume of water at p_{MAX}. The pressure vessel is a steel tank with an air cushion, the overall volume is $V_{PRESSURE\_VESSEL}$ (equal to 11 liters), the inner diameter is $d_{PRESSURE\_VESSEL}$ (equal to 17 cm), the cross-section is $S_{PRESSURE\_VESSEL}$ (equal to 227 cm^2), easily obtainable from the following relation:

$$S_{PRESSURE\_VESSEL} = \frac{\pi}{4} * d_{PRESSURE\_VESSEL}^{\ 2} \quad (2)$$

The height of the pressure vessel is $h_{PRESSURE\_VESSEL}$ (47 cm). The water supplied by the pump compresses the air cushion contained in the vessel until the pump stops when p_{MAX} is reached; actually, a part of the air mass in the cushion is then solubilized in the water through the air-liquid interface. Thus, the air mass inside the CAV decreases during the various system operating cycles (loading and unloading water).

The check valves allow one flow direction only.

The hoses connect different piping elements, the tank to the CAV, and the outlet port of the CAV back to the tank. This simplified configuration is used for simulation in the experimental lab equipment; in a real industrial case the outlet port is connected to the water distribution network covering the whole plant. Hoses have an overall length L=2 m and a diameter D=15 mm.

The monitoring system consists in a pressure sensor connected to air phase of the CAV, a flowmeter for the water flow on the outlet port, a level gauge measuring the water level in the CAV.

Water level is essential for the estimate of the air mass in the CAV; in fact, as the air mass decreases, the water level becomes higher with respect to the preset pressure values (respectively p_{MIN} and p_{MAX}). A combined measure of air pressure and water level is used by the controller to feedback the system during normal operating cycles (activating the pump) and gives an estimate of the decreasing trend of the air cushion (activating the air compressor or the air inlet valve to restore normal behavior).

3.3. Simulation model without mass transfer

The study of the transient operation of the pressure vessel starts with the modeling of the system and therefore with the determination of its parameters over time. In particular, the simulation model gives the current volumes of water (V_{WATER}) and air (V_{AIR}), both in liters; the air pressure (p_{AIR}), in absolute and relative atmospheres; the water flow at the outlet port and the delivery rate of the pump.

In a simplified case, in which the phenomenon of the air solubility is neglected, the following formula describes the air transformation in the CAV:

$$p_{AIR_{(t)}} * V_{AIR_{(t)}} = p_{AIR_{(t+1)}} * V_{AIR_{(t+1)}} \quad (3)$$

where *t* is a generic simulation step and *t+1* is the next step, simulation interval Δt between *t* and *t+1* is set to 1 second. As boundary condition, at the beginning of the simulation (*t=1*) p_{AIR} is set to atmospheric pressure (1 ata) and V_{WATER} to 3 liters.

For each simulation step, the model first calculates the $V_{AIR_{(t+1)}}$ [*l*], taking into account the volume of water $V_{PUMP_{(t+1)}}$ pumped inside the CAV during the simulation step; $V_{PUMP_{(t+1)}}$ is defined as the product of the supply flow rate of the pump Q_{PUMP} [*l/min*] multiplied by the time interval Δt.

In the same way the water volume $V_{USER_{(t+1)}}[l]$ at the outlet (i.e. the amount delivered to the distribution network) is computed as the product of the required flow Q_{USER} [*l/min*] and the considered time interval Δt.
The pump operates in on-off mode. It is activated when the air pressure inside the pressure vessel is lower than the minimum set point pressure (p_{MIN}=3 ata), while it stops whenever the air pressure reaches the maximum target value (p_{MAX}=4 ata). In particular, as shown in Figure 2 and Table 1, the delivery rate is not constant; rather, it varies according to the following equation (reported also in Table 2):

$$Q_{PUMP} = 0.08 * p_{OUTLET}^2 - 0.73 * p_{OUTLET} + 5.39 \quad (4)$$

The above relation is derived through an interpolation of Figure 2 and p_{OUTLET} is expressed in relative atmospheres (and it equals p_{AIR} inside the CAV). Equation 4 expresses the water flow entering the pressure vessel as a function of air pressure of the CAV, which is itself a function of time.

Table 2: pump delivery rate.

p_{OUTLET} (p_{AIR} of CAV)	Q_{PUMP} [l/h]	Q_{PUMP} [l/min]
2 atm	255	4.25
3 atm	235	3.92
4 atm	225	3.75

Another on-off system, using a valve as actuator, regulates the flow of water for the users Q_{USER} as a function of the time. When the valve is activated, it opens the flow section and the water flows from the CAV to the user (actually it goes back to the tank in our lab system). Given section 1 placed on the water surface of the pressure vessel, and section 2 at the end of the outlet pipeline, the following relation is used to estimate the water flow:

$$Q_{USER} = \sqrt{\frac{g*(z_1 - z_2) + \frac{p_1 - p_2}{\rho}}{R}} \quad (5)$$

Where:

- ρ is the density of water at 25°C (1,000 kg/m^3)
- g is the gravitational acceleration (9.81 m/s^2)
- R is an overall friction coefficient [m^{-4}] and can be derived applying Equation 6:

$$R = \frac{8*\lambda*L_{PIPE}}{\pi^2*D_{PIPE}^5} \quad (6)$$

R depends on the geometrical characteristics of the piping (hose and valves, length and diameter) and on a dimensionless friction coefficient λ, derived from the Reynolds number (*Re*) and set at 0.023. From this relationship and from the characteristics of the system it is possible to compute, for any time *t*, the water level z_1 [*cm*] inside the pressure vessel; this can be obtained as the ratio between the volume of water V_{WATER} and the cross section of the pressure vessel:

$$z_1 = \frac{V_{WATER}}{S_{PRESSURE\ VESSEL}} \quad (7)$$

For section 2, z_2=0, being the outlet pipe height set to the ground reference; p_1=p_{AIR} inside the pressure vessel and p_2=1 ata (atmospheric pressure).

3.4. Simulation model with mass transfer

In the real scenario, the solubility phenomenon of air cushion into the water takes place; thus, there is a variation over time of the air mass m_{AIR} [g] inside the vessel. In a generic time, the air mass consists mainly in the sum of the oxygen (O_2) and nitrogen (N_2) contributions, i.e.:

$$m_{AIR_{(t)}} = m_{O_{2_{(t)}}} + m_{N_{2_{(t)}}} \quad (8)$$

In atmosphere, m_{N_2} equals 79% of the air mass while m_{O_2} is approximately 21%, neglecting the mass percentages of the other elements, such as noble gases and CO_2.
Any variation of m_{AIR} has effects on the air pressure, according to the following relation, which is valid under the (realistic) hypothesis of an isothermal transformations:

$$\frac{p_{AIR(t)}*V_{AIR(t)}}{m_{AIR(t)}} = \frac{p_{AIR(t+1)}*V_{AIR(t+1)}}{m_{AIR(t+1)}} \quad (9)$$

It is possible to quantify the contributions of oxygen m_{O_2} and nitrogen m_{N_2} using their respective mass fractions w:

$$m_{O_2} = m_{AIR} * w_{O2} \quad (10)$$
$$m_{N_2} = m_{AIR} * w_{N2} \quad (11)$$

where w_{O2} and w_{N2} are the mass fractions of the two gases (i.e. w_{O2}=21% and w_{N2}=79% as previously mentioned).
According to Section 3.3, for any simulation step the air pressure is computed according to the available volume V_{AIR}. The model thus estimates the increase in the concentration of gases in the water as a function of the pressure of the vessel.
In every time interval Δt, a small part of m_{AIR} moves from the air cushion and dissolves in water, leading to the dissolution of oxygen and nitrogen:

$$m_{O_{2_{DISSOLVED_{(t+1)}}}} = C_{O_{2_{DISSOLVED_{(t+1)}}}} * V_{WATER_{(t)}} \quad (12)$$
$$m_{N_{2_{DISSOLVED_{(t+1)}}}} = C_{N_{2_{DISSOLVED_{(t+1)}}}} * V_{WATER_{(t)}} \quad (13)$$

where $C_{O2_{DISSOLVED_{(t+1)}}}$ and $C_{N2_{DISSOLVED_{(t+1)}}}$ are the concentrations, in [*mg/l*], of oxygen and nitrogen respectively in the simulation step *t+1*. In turn, these

concentrations depend on the simulation step and on the pressure p_{AIR}. Moreover, their values are governed by two variables, i.e. the Henry's law solubility constants K_H and the solubilization speed of oxygen and nitrogen in water. The Henry's constants depend on media, temperature and pressure; for the considered system they account for:

$K_{H,O2}$ at 25°C 756.7 [atm l mol^{-1}]
$K_{H,N2}$ at 25°C 1600 [atm l mol^{-1}]

At time *t+1*, the masses of O_2 and N_2 in the air cushion thus account for:

$$m_{O2_{(t+1)}} = m_{O2_{(t)}} - m_{O2\ DISSOVED_{(t+1)}} \quad (14)$$
$$m_{N2_{(t+1)}} = m_{N2_{(t)}} - m_{N2\ DISSOLVED_{(t+1)}} \quad (15)$$

The air mass therefore varies over time according to equations (14)-(15); concerning the water phase, since the volume V_{WATER} is known it is possible to derive the concentrations of O_2 and N_2 [*g/l*] according to the following equations:

$$C_{O2_{(t+1)}} = \frac{C_{O2_{(t)}} * V_{WATER} + C_{O2_{(1)}} * V_{PUMP}}{V_{WATER} + V_{PUMP}} + \frac{C_{O2\,DISSOLVED_{(t+1)}}}{1000} \quad (16)$$
$$C_{N2_{(t+1)}} = \frac{C_{N2_{(t)}} * V_{WATER} + C_{N2_{(1)}} * V_{PUMP}}{V_{WATER} + V_{PUMP}} + \frac{C_{N2\,DISSOLVED_{(t+1)}}}{1000} \quad (17)$$

The first part of the sum in the equations above represents the weighted average of the concentrations of O_2 and N_2 in the V_{WATER} stored in the pressure vessel at time *t* plus the volume added by the feeding pump in Δt. In fact, the pump introduces in the vessel a volume of water V_{PUMP} for which the concentration of oxygen and nitrogen is not the same as that of the liquid already contained. Rather, pumped water has a concentration of O_2 and N_2 given by the balance resulting in the tank at atmospheric conditions $C_{O2_{(1)}}$ and $C_{N2_{(1)}}$, described below.
The second term in equations (16)-(17) is the contribution involved by solubilization. To calculate the dissolved concentrations, it is first necessary to estimate the maximum allowed concentration for oxygen and nitrogen, according to the Henry's law of solubility:

$$C_{O2,MAX_{(t+1)}} = \frac{p_{(t+1)} * w_{O2}}{K_{H,O2}} * 31.99 \left[\frac{g}{mol}\right] \quad (18)$$
$$C_{N2,MAX_{(t+1)}} = \frac{p_{(t+1)} * w_{N2}}{K_{H,N2}} * 28.01 \left[\frac{g}{mol}\right] \quad (19)$$

The first term of the products is the mass fractions of O_2 and N_2, the pressures in absolute atmospheres, the molecular weights of O_2 and N_2 and, at denominator, the Henry constants for O_2 and N_2.
At the beginning of the simulation (*t*=1), the maximum concentrations of O_2 and N_2 are calculated at atmospheric conditions (1 ata):

$$C_{O2,MAX_{(1)}} = C_{O2_{(1)}} = \frac{1 * w_{O2}}{K_{H,O2}} * 31.99 \left[\frac{g}{mol}\right] \quad (20)$$
$$C_{N2,MAX_{(1)}} = C_{N2_{(1)}} = \frac{1 * w_{N2}}{K_{H,N2}} * 28.01 \left[\frac{g}{mol}\right] \quad (21)$$

Concerning the increase of concentration of gases in water, the speed of gas solubilization is proportional to the difference of concentrations and to the surface/volume ratio of the reactor where the phenomenon takes place:

$$n_{GAS} = k_L \frac{A}{V}(C^* - C_L) = k_L a (C^* - C_L) \quad (22)$$

where:

- k_L is the transfer coefficient of the liquid film [$m\ s^{-1}$];
- *A* and *V* are respectively equal to the gas-liquid exchange area and the volume of the reactor considered;
- *a* is the interface area (*A/V*) [$m^2\ m^{-3}$];
- $(C^*\text{-}C_L)$ is the concentration gradient [$mg\ l^{-1}$], also called "diving force";
- C^* is the maximum concentration (saturation solubility) of the considered gas in the liquid [$mg\ l^{-1}$];
- C_L is the current concentration, at time *t*, of the gas in the liquid [$mg\ l^{-1}$].

Each component of equation (22) has been evaluated for the specific case under examination. The product $k_L a$ is characteristic for every ventilation system with an air-liquid interface. The interfacial area *a* is given by the ratio between the surface area (*A*, which is $S_{PRESSURE\_VESSEL}$) and the volume (V_{WATER}); while the surface area is constant, the volume varies according to the quantities of water inside the CAV. An analysis of literature shows that k_L has to be experimentally determined for each specific system; to be more precise, the whole amount $k_L a$ should be investigated rather than the two terms (k_L and *a*) separately. Hence, to run the simulator, the following values were set for the case under examination, according to the literature (http://astratto.info/lacqua-ha-un-elevato-potere-solvente-verso-i-solidi-ionici-e-i.html):

$k_L\ O_2 = 2.72 * 10^{-6}$ m/s
$k_L\ N_2 = 2.72 * 10^{-6}$ m/s.

The execution of an experimental campaign, as a further development of the present work, could allow for a more precise estimate of the k_L coefficients for the system investigated.
Going back to the $C_{DISSOLVED}$ term in equations (16)-(17), the concentration of O_2 and N_2 dissolved in water at step *t+1* is determined as follows:

$$C_{O2_{DISSOLVED_{(t+1)}}} = k_{L,O2} a_t * \Delta t * (C_{O2,MAX} - C_{O2})_t \quad (23)$$
$$C_{N2_{DISSOLVED_{(t+1)}}} = k_{L,N2} a_t * \Delta t * (C_{N2,MAX} - C_{N2})_t \quad (24)$$

Equations (23)-(24) state that there is an increase in the liquid concentration for a specific gas only if the current concentration is lower than the maximum allowed concentration.

3.5. Model implementation and simulation strategy

The set of equations detailed in the previous subsections, linked together to reproduce the whole model developed, have been implemented in Microsoft Excel™ to build a simulation tool.
The objective of the tool is to describe the system under different working conditions. In particular, the model was run with a twofold aim: validating the model and estimating the mass transfer phenomena inside the vessel.
Regarding the first objective, the simulation outcomes depicted in Figures 3, 4 and 5 represent the trend of air pressure p_{AIR}, water level z_1, pump and water demand by the user (Q_{PUMP} and Q_{USER}) as a function of the time. These variables describe the macroscopic behaviour of the system, as pointed out in Section 3.3.
The second aim is the estimate of the mass transfer phenomena, described in Section 3.4. Figures 6 and 7 stress the variations of O_2 and N_2 concentrations in water (C_{O2} and C_{N2}), as well as their maximum allowed concentrations depending on p_{AIR} ($C_{O2,max}$ and $C_{N2,max}$). Finally, Figure 8 plots the O_2 and N_2 mass reduction in the CAV versus time, over a simulation time of 1 day and 216 loading cycles.
The results of the simulations are detailed in the section that follows.

4. RESULTS

Figure 3 depicts the trend in time of vessel pressure p_{AIR}, water level, pump operation (*on-off*) and users' water demand (Q_{USER} from 0 to 100%) during the initial operating activity of the CAV.

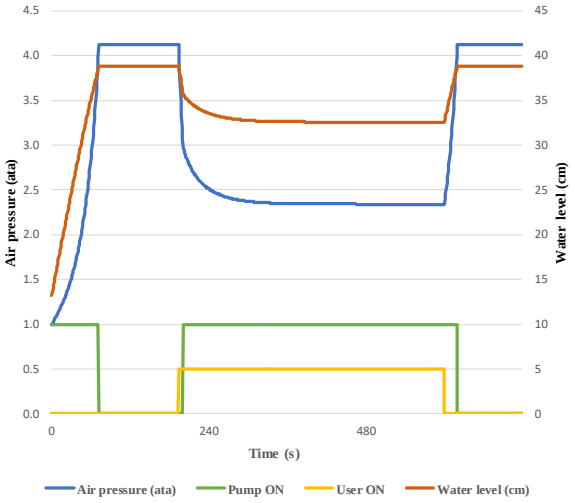

Figure 3: plot of vessel pressure, water level, pump operation and users' water demand versus time (simulation duration: 12 minutes).

The initial pressurizing phase is characterised by the water pump on, filling the vessel and reducing V_{AIR} until p_{MAX} is reached. Then a steady state with stable pressure is reached and maintained. When the distribution network requests a water flow set to 50% of Q_{MAX}, the vessel reacts by deflating the air cushion; hence, pressure drops and the water pump switches on to restore the pressurisation. A stable working point is found at about 2.3 ata; at this pressure, the water demand is balanced by the delivery rate of the pump. This state ends when the outlet valve is closed; at this point, pressure rises to p_{MAX} and, after some time, the pump is switched off as well.

Figure 4 reports the same plot over a longer time interval (1 h), where 5 loading cycles have been simulated.

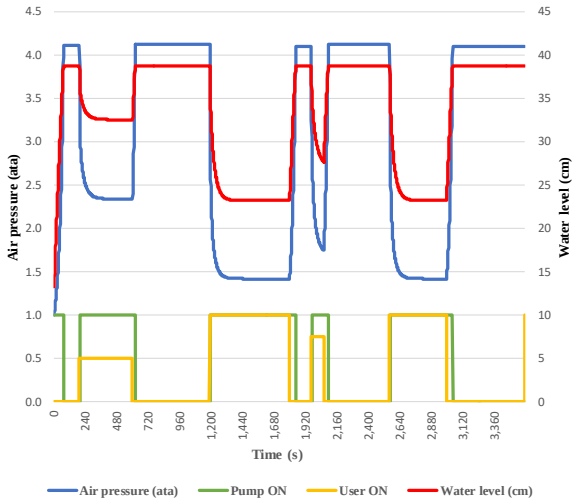

Figure 4: plot of vessel pressure, water level, pump operation and users' water demand versus time (simulation duration: 1 h).

Figure 5 focuses on the water flows of the pump and the distribution network, the latter simulated by means of a valve. The simulated scenario and conditions are the same as Figure 3; after the transient effect due to the output valve opening, the system finds a steady working condition where the two flows are perfectly balanced.

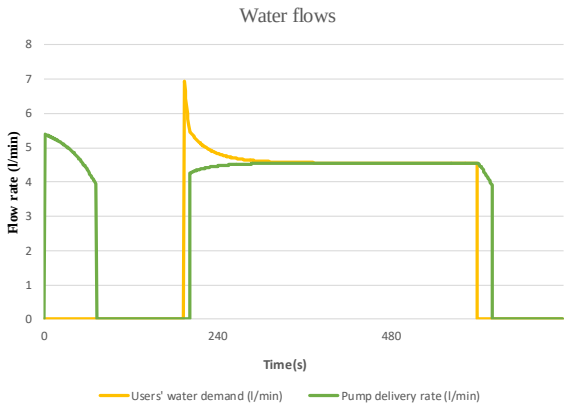

Figure 5: plot of users' water demand and pump delivery rate versus time (simulation duration: 12 minutes).

The above figures present the trend of the relevant variables which is, as a matter of facts, qualitatively confirmed by the physics underlying the problem. The next plots aim instead to investigate the hidden side of

the CAV, i.e. the mass transfer phenomenon, focusing on the behaviour of pressurised oxygen and nitrogen in the air cushion.

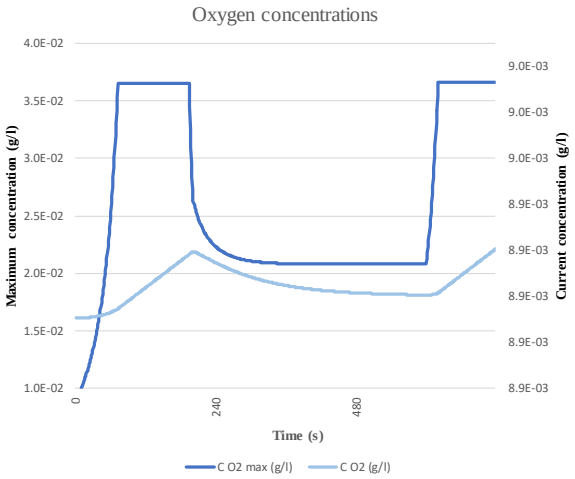

Figure 6: plot of oxygen maximum concentration in water $C_{02,MAX}$ and current concentration C_{02} versus time (initial phase, 12 minutes)

Figure 6 reports the trend of the oxygen concentrations in the first 12 minutes of system working. $C_{02,MAX}$ increases with pressure (according to the Henry's law) and the current concentration C_{02} increases as well, although it is always lower than $C_{02,MAX}$. This is consistent with the fact that the driving force $C_{O2,MAX} - C_{O2}$ is responsible for the mass transfer (see equation 23). The same behaviour can be observed in Figure 7, where the nitrogen concentrations $C_{N2,MAX}$ and C_{N2} have been added; the simulation duration in this figure has been extended to 1 h.

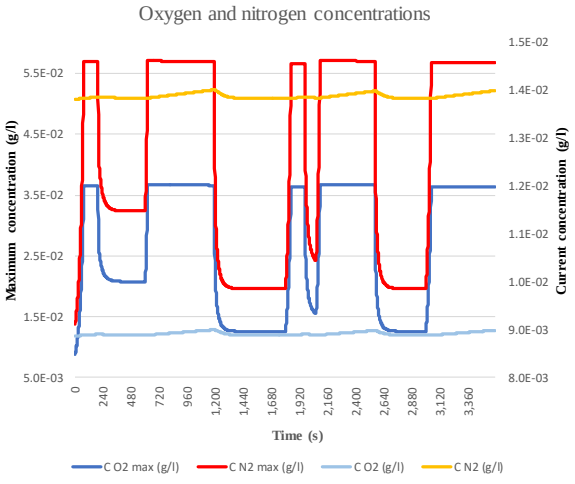

Figure 7: plot of oxygen and nitrogen maximum and current concentrations versus time (simulation duration: 1 h).

In order to observe the reduction of the trapped air in the air cushion, the simulator has been tested on multiple loading/unloading cycles. More in details, 216 cycles have been simulated; each cycle is composed of a loading phase of 200 seconds (Q_{USER}=0) followed by a unloading phase of 200 seconds (Q_{USER}=100% as per equation 5). The overall simulated time is 86,400 seconds corresponding to 1 working day. During each cycle, a small quantity of gas dissolves in water, as pointed out in Figure 8. Oxygen mass, taken as an example, decreases from 2.18 g to 2.10 g, corresponding to a 3.6% reduction.

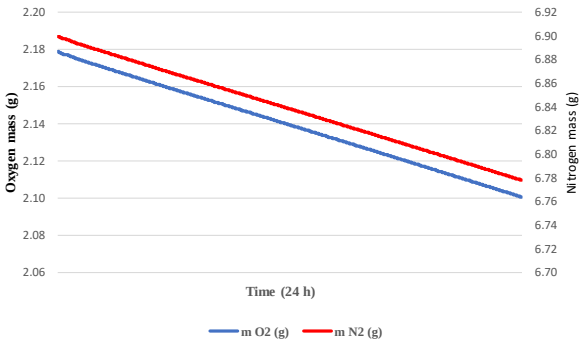

Figure 8: plot of oxygen and nitrogen mass reduction in the CAV versus time (simulation duration: 1 day, 216 load/unload cycles)

This phenomenon cannot be observed and detected by simply controlling the pressures values (p_{MIN} and p_{MAX}) because the system automatically reacts to the air mass loss by replacing it with water. This means that, although the air mass decreases in time, the pressure vessel still works correctly between p_{MIN} and p_{MAX}. The user can detect the air loss by observing an increase in the water level corresponding to p_{MAX} and some changes in the on-off cycles of the pump. More precisely, their frequency increases while the duration of the on-phase decreases.

5. CONCLUSIONS

The model developed in this paper, built in Microsoft Excel™, considers both the compression of the air cushion according to the volume of water contained into the vessel and the mass transfer phenomenon, whose rate depends on temperature and pressure. Nitrogen and oxygen contributions have been separately considered, due to their different behaviour.

Today's systems installed and running are based on negative feedback systems, whose closed loops separately control the water feeding pump (according to the pressure measured in the vessel) and the compressed air inlet valve (according to the measured water level at a given pressure). This system works fine although it is blindfolded: it just reacts to the current measured variables and does not care about their trend and history. On the contrary, thanks to the adoption of the proposed predictive model, a microcontroller or a PLC managing the system can also be able to detect possible failures before they happen and compromise the functionality of the system itself. In fact, predictive modelling can predict outcomes, such as the value of given variables, according to the state of the system. Most often the event one wants to predict is in the future, but predictive modelling can be applied to any type of unknown event, regardless of when it occurred. For example, predictive models can be used

to compare the current value of pressure, or water level in the vessel, with predicted ones, according to the previous state of the system and the other measured variables. In case the match is not positive, within a certain tolerance, something has occurred and the failure might be approaching.

The results obtained in this paper allow to conclude that the model can act as an enabler of pro-active system monitoring, as it allowed for many system variables to be predicted in time. Nonetheless, some steps are still needed. In particular, results need to be validated by comparing them with those obtained (for instance) using a CFD software. Moreover, as soon as the lab equipment described is up and running, the model can be validated with experimental data acquired from the real pressure vessel. The same considerations hold true for the mass transfer coefficients used in this paper, which were taken from literature but not directly measured; they could be confirmed by in-field experiments.

REFERENCES

Besharat, M., Tarinejad, R., Taghi Aalami, M., Ramos, H. M. (2016). "Study of a Compressed Air Vessel for Controlling the Pressure Surge in Water Networks: CFD and Experimental Analysis", Water Resource Manage, 30, 2687–2702;

Besharat, M., Viseu, M. T., Ramos, H. M. (2017). "Experimental Study of Air Vessel Behavior for Energy Storage or System Protection in Water Hammer Events", Water, 9(1), 63;

Ivljanin, B., Stevanovic, V. D., Gajic, A. (2018). "Water hammer with non-equilibrium gas release", International Journal of Pressure Vessels and Piping, 165, 229–240;

Okayama, A., Nakamura, O., Higuchi, Y. (2018). "Analysis of Plunging Pool Formation and Gas Absorption Phenomenon during Tapping", ISIJ International, 58, 4;

Vlyssides, A., Barampouti, E. M., Mai, S. (2003). "Kinetics of Air Absorption by Water in Sparged Agitated Pressure Vessels", Industrial & Engineering Chemistry Research, 42(24), 6323 – 6235.

Zhou, L., Liu, D., Karney, B., Zhang, Q. (2011). "Influence of Entrapped Air Pockets on Hydraulic Transients in Water Pipelines", Journal of Hydraulic Engineering, 137(12), 1686-1692;

AUTHORS BIOGRAPHY

Eleonora BOTTANI is Associate professor in Mechanical Industrial Plants at the Department of Engineering and Architecture of the University of Parma since September 2014. She graduated (with distinction) in Industrial Engineering and Management in 2002 and got her Ph.D. in Industrial Engineering in 2006, both at the University of Parma. Her primary research activities concern logistics and supply chain management issues; secondary topics encompass industrial plants and food plants. She is author (or co-author) of more than 170 scientific papers (H-index=19), referee for more than 60 international journals, editorial board member of five scientific journals, Associate Editor for one of those journals, and editor-in-chief of a scientific journal.

Andrea VOLPI graduated in July 2003 in Mechanical Engineering at the University of Parma. Since January 2006, he has been working as Ph.D. student in Industrial Engineering Department at the same University. His major activities have been devoted to managing the research projects carried out in RFID Lab, a forefront laboratory in the same department. Since November 2015, he works as Associate Professor at University of Parma, and his research activities are mainly concerned with logistics, supply chain and operation management; thus his skills and competences are mainly related to RFID and logistics topics which are expressed in many papers produced. He acts as a referee for some international scientific journals, such as International Journal of RF Technology: Research and Applications, International Journal of Logistics: Research and Applications.